2015

Energetics, structure, and rovibrational spectroscopic properties of the sulfurous anions SNO^- and OSN^-

Ryan C. Fortenberry
Georgia Southern University, r410@olemiss.edu

Joseph S. Francisco
University of Nebraska-Lincoln, frjoseph@sas.upenn.edu

Energetics, structure, and rovibrational spectroscopic properties of the sulfurous anions SNO^- and OSN^-

Ryan C. Fortenberry[1,a)] and Joseph S. Francisco[2,b)]
[1]*Department of Chemistry, Georgia Southern University, Statesboro, Georgia 30460, USA*
[2]*Department of Chemistry, University of Nebraska-Lincoln, Lincoln, Nebraska 68588, USA*

(Received 25 September 2015; accepted 21 October 2015; published online 9 November 2015)

The SNO^- and OSN^- anions are shown in this work to be very stable negatively charged species in line with other recent work [T. Trabelsi *et al.*, J. Chem. Phys. **143**, 164301 (2015)]. Utilizing established quartic force field techniques, the structural and rovibrational data for these anions are produced. The SNO^- anion is less linear and has weaker bonds than the corresponding neutral radical giving much smaller rotational constants. OSN^- is largely unchanged in these regards with inclusion of the additional electron. The S–N bond is actually stronger, and the rotational constants of OSN^- versus OSN are similar. The vibrational frequencies of SNO^- are red-shifted from the radical while those in OSN^- are mixed. OSN^- has mixing of the stretching modes while the S–N and N–S stretches of SNO^- are largely independent of one another. The ω_3 stretches are much brighter in these anions than they are in the radicals, but the ω_1 stretches are still the brightest. © *2015 AIP Publishing LLC.* [http://dx.doi.org/10.1063/1.4935056]

I. INTRODUCTION

It is surprising that so very little is known about the simple triatomic singlet anion, SNO^-, and its isomer, OSN^-. Interest in these anions and their corresponding neutral radicals has grown very recently due to their perceived importance in atmospheric, planetary (Venus, in particular), circumstellar, and interstellar contexts.[1–5] However, the literature is bereft of data on these anions from before 2015. The neutral radicals have been studied for over 40 years,[6–11] but exhaustive analysis of the reaction, electronic, and rovibrational physics of these systems has only recently emerged.[1–3,12] There still exists controversy as to the attribution of vibrational features arising from the $2\nu_3$ overtone and ν_1 fundamental band in the 1500 cm^{-1} to 1650 cm^{-1} range.[1,2] The very bright nature of the SNO ν_1 band compared to the lesser $2\nu_3$ intensity will allow for conclusive assignment of the bands once gas-phase experiments on this system can be undertaken.

Anions have been detected in various astronomical sources[13–22] since 2006 when the rotational spectrum of C_6H^- was teased out of observations of the carbon-rich star IRC + 10 216.[13] The smallest of these known anions, CN^-, is believed to form in space from collisional processes,[23] but the larger anions likely form via dipole-bound formation pathways.[18,24] It has been proposed that some large anions of interest to astrochemistry may be present in interstellar or circumstellar media,[25] but it has also been discussed that longer, molecular chain anions of the type observed in various astronomical environments are not likely to be detected.[24] Consequently, small anions like those examined in this work are good candidates for growing the astronomically observed anion population.

The anion form of sulfur-substituted nitrogen dioxide is stable in both the SNO^- and OSN^- isomers. Very recent work shows that OSN^- is more stable than SNO^- by roughly 1 eV in contrast to the neutral radicals where OSN is only 0.12 eV more stable than SNO.[1–3] This is, at surface level, a somewhat surprising result since the analogous standard O–N–O isomer of NO_2 is more stable than the peroxy N–O–O form of the analogue.[26] However, the nature of sulfur bonding[27–29] promotes a more energetically favorable environment with it as the central atom in the molecule in a fashion akin to standard SO_2.[2] Furthermore, SO_2 has the same number of electrons as SNO^- making the two isoelectronic with one another, and the electronic arrangement of OSN^- is of the same type as SO_2 making this pair of molecules isovalent. The potential energy surface cuts and electronic descriptions of these two anion isomers are given in Ref. 3 providing a clear indication that the $^1A'$ states are the lowest energy electronic configurations for these systems and barriers to dissociation are also well into the UV range at greater than 3 eV and 5 eV in most cases. Hence, these anions are excellent candidates for rovibrational analysis due to their deep wells and relatively high stabilities as far as anions are concerned.

An efficient yet accurate means of describing spectroscopic quantities and vibrational frequencies has been showcased through the use of quartic force fields (QFFs).[30] QFFs are fourth-order Taylor series expansions of the potential portion within the internuclear Hamiltonian. Composite energy schemes to describe the QFF surface developed by Lee and Huang at NASA Ames[31–34] have been able to match experimental fundamental vibrational frequencies to within 1.0 cm^{-1} of experiment in many cases[33,35–39] and within 0.03 Å for bond lengths and 10–20 MHz for some experimental B- and C-type rotational constants.[33,34,37,40,41] In fact, QFFs have even shown reliability in the provision of rovibrational insights for closed-shell anions,[24,41–47] much like SNO^- and OSN^-, most notably in the interstellar detection of C_5N^- which was based solely on quantum chemical spectroscopic data.[19,48] These same techniques are applied here to the SNO^- and OSN^-

a)rfortenberry@georgiasouthern.edu
b)jfrancisco3@unl.edu

anion isomers in order to offer the community deeper insights into the rotational, vibrational, and rovibrational character of these stable and simple inorganic species. Understanding of interstellar anion chemistry is growing,[21,22,24,49,50] and more data on potential interstellar anions such as SNO^- and OSN^- will help in enriching the depth of information for this class of molecules.

II. COMPUTATIONAL DETAILS

Following from the reliable QFF methodology established previously,[31–34] the SNO^- and OSN^- geometries are optimized with restricted Hartree-Fock reference wave functions[51] and the coupled cluster singles, doubles, and perturbative triples [CCSD(T)][52] level of theory with the aug-cc-pV5Z (aug-cc-pV(5+d)Z for sulfur) basis set.[53,54] Corrections for inclusion of core electron correlation augment these geometries and are treated as the additive difference in geometrical parameters computed with the Martin-Taylor (MT) core correlating basis set[55] for optimizations with and without inclusion of core electrons. From these reference geometries, grids of 129 symmetry-unique points are generated for each isomer in the same way that they have been done for other C_s, triatomic species.[2,56–58] Coordinate 1 is the S–N stretch in SNO^- and the O–S stretch in OSN^-; coordinate 2 is the N–O stretch in SNO^- and the S–N stretch in OSN^-; and coordinate 3 is the bend for both species. All computations make use of the MOLPRO 2010.1 quantum chemistry program[59] except the MP2/6-31+G* double harmonic intensities produced from the Gaussian09 program.[60–62]

At each point, CCSD(T) energies are computed with the aug-cc-pVTZ, aug-cc-pVQZ, and aug-cc-pV5Z basis sets with the $(X + d)$ functions included for sulfur. These energies are extrapolated to the complete basis set (CBS) limit via a three-point formula[63] to give the "C" term. Additive corrections for the difference in the CCSD(T)/MT energies with and without core electrons provide the "cC" term. Similar additive, difference corrections for scalar relativity[64] generate the "R" term. Each of these seven energy computations at each of the 129 points creates the CcCR QFF. These points are then fitted via a least-squares method to produce the final CcCR equilibrium geometry. Refitting these points gives zero gradients and proper force constants for the Taylor series expansion of the potential in the internuclear Hamiltonian. Transforming the coordinates from simple-internal to Cartesian definitions is accomplished via the INTDER program.[65] Second-order perturbation theory for rotational[66] and vibrational (VPT2)[67,68] computations employs these derivatives within the SPECTRO program[69] to produce the rotational constants and vibrational frequencies. Input of resonances is possible for SPECTRO. SNO^- requires a $2\nu_3 = \nu_2 + \nu_3 = \nu_1$ Fermi resonance polyad while OSN^- dictates inclusion of a $2\nu_2 = \nu_3$ type-1 Fermi resonance. These are consistent across isotopologues.

TABLE I. $[S,N,O]^{\cdot/-}$ CcCR energy matrix (in eV) relative to OSN^-.

	OSN^-	SNO^-	OSN
SNO^-	1.12		
OSN	3.16	2.04	
SNO	3.28	2.16	0.12

III. RESULTS AND DISCUSSION

A. Relative energies

The $\tilde{X}^1A'$ states of SNO^- and OSN^- are formed by doubly occupying the singly occupied highest molecular orbital $(12a')$ within the radicals.[3] The lower-mass analogues, ONO^- (nitrite) and NOO^-, are known stable species that have a similar valence orbital construction.[26] The highly descriptive CcCR relative equilibrium energies for OSN and SNO (from Ref. 2) as well as the corresponding anions determined in this work are

TABLE II. The simple-internal CcCR force constants (in mdyn/Å^n rad^m) for SNO^-.

F_{11}	4.105 993	F_{221}	13.4809	F_{1111}	62.96	F_{3222}	294.87
F_{21}	−2.845 601	F_{222}	−32.8391	F_{2111}	31.60	F_{3311}	330.33
F_{22}	6.472 398	F_{311}	−15.7622	F_{2211}	−23.52	F_{3321}	−513.49
F_{31}	−2.602 456	F_{321}	37.3335	F_{2221}	−13.20	F_{3322}	636.01
F_{32}	9.044 425	F_{322}	−63.0237	F_{2222}	98.97	F_{3331}	−1120.29
F_{33}	22.147 669	F_{331}	91.1590	F_{3111}	−26.82	F_{3332}	1013.73
F_{111}	−14.996 1	F_{332}	−116.9822	F_{3211}	69.85	F_{3333}	805.92
F_{211}	−4.731 5	F_{333}	−195.1452	F_{3221}	−167.26		

TABLE III. The OSN^- CcCR QFF simple-internal force constants (in mdyn/Å^n rad^m).

F_{11}	10.249 395	F_{221}	22.0415	F_{1111}	244.09	F_{3222}	270.22
F_{21}	−4.825 471	F_{222}	−39.3822	F_{2111}	12.67	F_{3311}	329.18
F_{22}	7.429 658	F_{311}	−29.5152	F_{2211}	11.41	F_{3321}	−381.03
F_{31}	−5.152 049	F_{321}	44.0152	F_{2221}	−61.33	F_{3322}	381.03
F_{32}	9.133 960	F_{322}	−58.7403	F_{2222}	141.83	F_{3331}	−505.59
F_{33}	16.887 853	F_{331}	71.8921	F_{3111}	−81.21	F_{3332}	343.08
F_{111}	−43.236 7	F_{332}	−78.1656	F_{3211}	133.64	F_{3333}	−122.38
F_{211}	−10.670 5	F_{333}	−87.1096	F_{3221}	−202.01		

TABLE IV. The SNO^- equilibrium and zero-point (R_α) geometries, vibrational frequencies and intensities,[a] and spectroscopic constants from the CcCR QFF.

	SNO^-	Previous[b]	$^{34}SNO^-$	$S^{15}NO^-$	$SN^{18}O^-$
r_0 (S–N) Å	1.706 947		1.706 859	1.706 828	1.706 973
r_0 (N–O) Å	1.225 753		1.225 830	1.225 896	1.225 872
∠(S–N–O)	118.047		118.046	118.048	118.049
A_0 cm^{-1}	3.144 587		3.137 652	2.996 888	3.059 307
B_0 cm^{-1}	0.227 293		0.221 389	0.226 308	0.214 391
C_0 cm^{-1}	0.211 637		0.206 475	0.210 077	0.200 044
A_1 cm^{-1}	3.116 695		3.108 627	2.969 360	3.033 175
B_1 cm^{-1}	0.227 076		0.221 188	0.226 122	0.214 131
C_1 cm^{-1}	0.211 395		0.206 247	0.209 855	0.199 781
A_2 cm^{-1}	3.168 425		3.159 518	3.018 861	3.081 544
B_2 cm^{-1}	0.226 641		0.220 742	0.225 655	0.213 835
C_2 cm^{-1}	0.210 792		0.205 653	0.209 216	0.199 315
A_3 cm^{-1}	3.175 293		3.168 205	3.024 510	3.086 053
B_3 cm^{-1}	0.225 839		0.219 992	0.224 891	0.213 012
C_3 cm^{-1}	0.210 135		0.205 023	0.208 635	0.198 604
D_J kHz	4.321		4.122	4.264	3.831
D_{JK} kHz	−70.142		−70.142	−63.875	−70.357
D_K MHz	5.256		5.487	4.998	5.277
d_1 kHz	−0.435		−0.405	−0.445	−0.379
d_2 Hz	−21.622		−19.715	−23.253	−18.006
H_J mHz	0.306		0.251	0.164	0.504
H_{JK} Hz	−0.217		−0.202	−0.211	−0.183
H_{KJ} Hz	−24.819		−24.015	−21.801	−23.212
H_K kHz	1.116		1.104	0.961	1.041
h_1 mHz	0.763		0.693	0.751	0.661
h_2 mHz	0.086		0.077	0.090	0.069
h_3 mHz	0.019		0.016	0.021	0.015
r_e (S–N) Å	1.700 936	1.706	…	…	…
r_e (N–O) Å	1.234 698	1.238	…	…	…
∠(S–N–O)	118.054	117.9	…	…	…
A_e MHz	3.133 761		3.125 955	2.985 856	3.047 883
B_e MHz	0.228 456		0.222 512	0.227 436	0.215 488
C_e MHz	0.212 932		0.207 726	0.211 338	0.201 259
μ_x D	−0.35		…	…	…
μ_y D	0.10		…	…	…
μ[c] D	0.36		…	…	…
Harmonic zero-point cm^{-1}	1304.3		1299.65	1281.6	1277.8
ω_1 cm^{-1} N–O	1366.8 (531)	1363.9	1366.6	1343.3	1329.6
ω_2 cm^{-1} bend	497.6 (8)	495.4	491.7	495.0	484.6
ω_3 cm^{-1} N–S	744.3 (257)	742.8	741.0	724.9	741.4
Zero-point cm^{-1}	1298.9		1294.3	1276.4	1272.6
ν_1 cm^{-1} N–O	1336.1		1335.6	1313.5	1301.3
ν_2 cm^{-1} bend	490.9		485.2	488.4	478.2
ν_3 cm^{-1} N–S	733.0		729.9	714.2	729.9
$2\nu_1$ cm^{-1}	2649.6		2649.2	2605.4	2580.1
$2\nu_2$ cm^{-1}	978.9		967.4	973.9	953.8
$2\nu_3$ cm^{-1}	1459.3		1453.5	1422.3	1452.2
$\nu_1+\nu_2$ cm^{-1}	1828.9		1823.1	1803.8	1780.4
$\nu_1+\nu_3$ cm^{-1}	2075.8		2072.2	2034.2	2037.5
$\nu_2+\nu_3$ cm^{-1}	1217.6		1208.8	1196.5	1201.8
α^A 1 MHz	866.2		870.2	825.3	783.4
α^A 2 MHz	−684.7		−655.5	−658.7	−666.6
α^A 3 MHz	−890.6		−916.0	−828.1	−801.8
α^B 1 MHz	6.5		6.0	5.6	7.8
α^B 2 MHz	19.6		19.4	19.6	16.7

TABLE IV. (*Continued.*)

	SNO^-	Previous[b]	$^{34}SNO^-$	$S^{15}NO^-$	$SN^{18}O^-$
α^B 3 MHz	43.6		41.9	42.5	41.3
α^C 1 MHz	7.3		6.8	6.6	7.9
α^C 2 MHz	25.4		24.6	25.8	21.8
α^C 3 MHz	45.3		43.5	43.2	43.2

[a]The MP2/6-31+G* double harmonic intensities are in parentheses beside the harmonic frequency of the standard isotopologue and given in km/mol.
[b]CCSD(T)-F12/aug-cc-pVQZ-F12 results from Ref. 3.
[c]The SNO coordinates (in Å with the center-of-mass at the origin) used to generate the CCSD(T)/aug-cc-pVTZ Born-Oppenheimer dipole moment component are S, −1.009 541, 0.084 540, 0.000 000; N, 0.579 433, −0.522 374, 0.000 000; O, 1.510 684, 0.288 337, 0.000 000.

given in Table I relative to OSN^-, the lowest energy species. SNO^- lies 1.12 eV above, in line with the work from Trabelsi and co-workers.[3] The adiabatic electron binding energy (eBE), an equivalent but more informative description of the standard electron affinity for neutrals,[70] differs somewhat here for the CcCR values from those determined previously.[3] The OSN^- eBE, 3.16 eV, is 0.35 eV below the 3.51 eV adiabatic value computed from CCSD(T)-F12/aug-cc-pVQZ-F12 previously but in line with the 3.10 eV vertical value. The SNO^- CcCR eBE is 2.16 eV, notably below the previous 2.75 eV adiabatic value but well above the 1.35 eV vertical value.[3] The same qualitative trends are present, in either case, showing that the OSN^- and SNO^- anions are also very stable systems.

The previous work[1,2] has indicated that dipole-bound excited states of these anions[24,50,71] are not likely due to the relatively small dipole moments of the neutral radicals, i.e., ≤2.0 D. Consequently, their formation in the ISM would have to come from collisional or reactive means[12] in a fashion similar to the interstellar formation of CN^-,[20,23] another stable, small, closed-shell anion. This is in opposition to the perceived dipole-bound anion formation hypothesis growing in evidence as to the provenance of, at least, the known polyyne and cyanopolyyne carbon chain anions larger than CN^-.[18,23,24] However, such processes are still likely in natural environments and can certainly be manipulated in the laboratory for the synthesis of these anions.

B. Molecular structures and spectroscopic constants

The first thing of note regarding the structures of SNO^- and OSN^- is the significant decreases in the diagonal, harmonic force constants for SNO^- given in Table II; these values are proportional to the bond strengths. Compared to those of the radical,[2] the S–N and N–O bonds are weaker by 41.4% and 37.3%, respectively. In contrast, the OSN^- F_{11} value given in Table III has a much smaller decrease of less than 1.0 mdyn/Å^2 for the O–S bond to 10.249 395 mdyn/Å^2. Interestingly, the S–N bond actually strengthens in the OSN^- structure increasing the F_{22} value from 6.000 068 mdyn/Å^2 to 7.429 658 mdyn/Å^2.

These inferences regarding changes in the bond strengths are supported by the differences in the vibrationally averaged (R_α) structures between the radical and the anion with the latter given in Tables IV and V. The S–N bond in SNO^- is more than 0.1 Å longer than the neutral at 1.706 947 Å with the N–O bond 0.03 Å longer at 1.225 753 Å. The bond angles are also drastically different with the anions much smaller at 118.047°. The equilibrium geometries closely corroborate previous CCSD(T)/aug-cc-pV6Z and, specifically, CCSD(T)-F12/aug-cc-pVQZ-F12 values determined by Trabelsi and co-workers.[3] The O–S bond in OSN^- is 0.05 Å longer at 1.499 999 Å in the anion than in OSN which follows from the slight increase in F_{11} for the anion over the radical. The anion's S–N bond shortens (1.463 718 Å) for the related but inverted reason since the S–N bond is stronger in the anion than in the corresponding radical.

As a result of the bond angle and the subsequent linear character decreasing in SNO^- as compared to SNO, the *A*-type, vibrationally averaged rotational constant in Table IV decreases by more than 50% to 3.144 587 cm^{-1} while the *B*- and *C*-type constants are not affected as drastically. Since the bond angles and bond lengths of OSN^- are similar to OSN, the rotational constants for this anion are quite similar to the corresponding neutral radical. Even though the *A*-type rotational constants for SNO^- are significantly less than in the corresponding neutral-radical, they are still 0.9 cm^{-1} greater than their counterparts in OSN^-.

Single-inclusion of the ^{34}S, ^{15}N, and ^{18}O isotopes shifts the geometrical parameters slightly, but these effects are more easily observed in the rotational constants than in comparison of the structures. The isotopologues are affected more by inclusion of ^{15}N and ^{18}O than ^{34}S since changes in the smaller masses are magnified when additional neutrons are considered in each nucleus. The vibrationally excited rotational constants for all isotopologues including the standard forms are also provided in Tables IV and V since the Atacama large millimeter array has come online and the resolution of astronomically observed vibrationally excited rotational peaks is now possible.[19] The quartic and sextic distortion constants are also given in Tables IV and V in order to characterize fully the rotational spectra of the SNO^- and OSN^- anions.

The CCSD(T)/aug-cc-pV5Z dipole moments for these molecules are computed from the CcCR center-of-mass equilibrium geometries. SNO^- is weakly dipolar with a strength of only 0.36 D, half of that from the corresponding neutral. The dipole moment vector is visually depicted in Fig. 1. The vector for the radical points more strongly toward the oxygen atom than here in the anion. The reduction in the dipole moment, especially in the μ_x component, results from a balancing of the negative partial charges between the sulfur and oxygen atoms in the anion as opposed to a partial positive on the sulfur

TABLE V. The CcCR QFF OSN^- equilibrium and zero-point (R_α) geometries, vibrational frequencies and intensities,[a] and spectroscopic constants.

	OSN^-	Previous[b]	$^{18}OSN^-$	$O^{34}SN^-$	$OS^{15}N^-$
r_0 (O–S) Å	1.499 999		1.499 831	1.499 953	1.499 974
r_0 (S–N) Å	1.463 718		1.463 924	1.463 776	1.463 820
∠(O–S–N)	123.757		123.754	123.757	123.757
A_0 cm^{-1}	2.248 475		2.191 186	2.184 665	2.205 492
B_0 cm^{-1}	0.327 111		0.307 918	0.327 087	0.316 319
C_0 cm^{-1}	0.284 850		0.269 329	0.283.772	0.275 962
A_1 cm^{-1}	2.226 909		2.170 493	2.164 279	2.184 123
B_1 cm^{-1}	0.325 887		0.306 811	0.325 882	0.315 126
C_1 cm^{-1}	0.283 703		0.268 277	0.282 644	0.274 853
A_2 cm^{-1}	2.299 146		2.239 248	2.233 794	2.254 398
B_2 cm^{-1}	0.327 206		0.308 007	0.327 176	0.316 414
C_2 cm^{-1}	0.284 313		0.268 843	0.283 228	0.275 457
A_3 cm^{-1}	2.249 381		2.192 459	2.184 835	2.207 031
B_3 cm^{-1}	0.325 288		0.306 209	0.325 828	0.314 592
C_3 cm^{-1}	0.283 349		0.267 920	0.282 299	0.274 529
D_J kHz	6.267		5.606	6.223	5.870
D_{JK} MHz	−0.129		−0.119	−0.123	−0.124
D_K MHz	4.002		3.788	3.779	3.856
d_1 kHz	−1.482		−1.288	−1.501	−1.377
d_2 kHz	−0.073		−0.063	−0.076	−0.067
H_J mHz	8.827		7.230	8.769	8.081
H_{JK} Hz	−0.389		−0.314	−0.394	−0.351
H_{KJ} Hz	−28.948		−26.128	−26.876	−27.270
H_K Hz	787.557		725.721	722.766	744.450
h_1 mHz	4.623		3.796	4.621	4.197
h_2 mHz	0.496		0.415	0.503	0.442
h_3 mHz	0.246		0.191	0.261	0.216
r_e (O–S) Å	1.495 038	1.498	…	…	…
r_e (S–N) Å	1.472 249	1.476	…	…	…
∠(O–S–N)	123.729	123.7	…	…	…
A_e MHz	2.233 469		2.176 865	2.170 209	2.190 953
B_e MHz	0.328 586		0.309 279	0.328 546	0.317 729
C_e MHz	0.286 444		0.270 804	0.285 347	0.277 488
μ_x D	−0.96		…	…	…
μ_y D	−1.78		…	…	…
μ[c] D	2.04		…	…	…
Harmonic zero-point cm^{-1}	1401.5		1377.0	1388.7	1383.6
ω_1 cm^{-1} antisym.	1299.9 (351)	1296.7	1296.1	1285.6	1275.5
ω_2 cm^{-1} bend	488.2 (31)	485.7	478.9	483.9	482.0
ω_3 cm^{-1} sym.	1015.0 (216)	1014.5	979.0	1007.8	1009.6
Zero-point cm^{-1}	1395.6		1371.3	1382.9	1377.8
ν_1 cm^{-1} antisym.	1280.2		1276.6	1266.4	1256.5
ν_2 cm^{-1} bend	483.0		473.9	478.8	477.0
ν_3 cm^{-1} sym.	999.4		964.5	992.4	994.2
$2\nu_1$ cm^{-1}	2546.1		2538.6	2518.7	2499.6
$2\nu_2$ cm^{-1}	965.1		946.9	956.7	953.1
$2\nu_3$ cm^{-1}	1988.3		1918.9	1974.3	1978.5
$\nu_1+\nu_2$ cm^{-1}	1759.7		1747.2	1741.8	1729.9
$\nu_1+\nu_3$ cm^{-1}	2272.6		2235.5	2252.3	2242.8
$\nu_2+\nu_3$ cm^{-1}	1479.0		1435.5	1467.9	1467.8
α^A 1 MHz	646.5		620.4	611.2	640.6
α^A 2 MHz	−1519.1		−1440.9	−1472.9	−1466.2
α^A 3 MHz	−27.2		−38.2	−5.1	−46.1
α^B 1 MHz	36.7		33.2	36.2	35.8
α^B 2 MHz	−2.8		−2.7	−2.7	−2.9

TABLE V. (*Continued.*)

	OSN^-	Previous[b]	$^{18}OSN^-$	$O^{34}SN^-$	$OS^{15}N^-$
α^B 3 MHz	54.7		51.2	54.1	51.8
α^C 1 MHz	34.4		31.5	33.8	33.3
α^C 2 MHz	16.1		14.6	16.3	15.1
α^C 3 MHz	45.0		42.2	44.3	43.0

[a]The MP2/aug-cc-pVTZ double harmonic intensities are in parentheses beside the harmonic frequency of the standard isotopologue and given in km/mol.
[b]CCSD(T)-F12/aug-cc-pVQZ-F12 results from Ref. 3.
[c]The OSN coordinates (in Å with the center-of-mass at the origin) used to generate the CCSD(T)/aug-cc-pVTZ Born-Oppenheimer dipole moment component are O, −1.253 973, 0.328 635, 0.000 000; S, 0.034 651, −0.325 084, 0.000 000; N, 1.353 225, 0.366 855, 0.000 000.

and partial negative on the oxygen within the radical. This is in line with the molecular orbitals produced in Ref. 3. The μ_y components are small in both the radical and anion but contribute more in the latter. As a result, the dipole moment of the anion is not nearly as closely aligned with the *A* axis as it is for the radical.

OSN^- is more strongly dipolar at 2.04 D than SNO^- and has a similar vector direction as shown in Fig. 2 from a connectivity perspective in that the dipole vector seemingly bisects the molecule. The rotational constants shift for OSN^- as compared to SNO^- putting the dipole vector almost exclusively along the *A* rotational axis. The OSN^- dipole moment vector differs from its corresponding radical where that of the latter points more toward the oxygen atom and is nearly half the magnitude. The partial charges of the nitrogen and oxygen atom are more balanced in the anion than the radical creating an electronic environment nearly truly isovalent to that of SO_2. The greater stability of OSN^- compared to SNO^-, combined with its significantly larger dipole moment, should make it more easily rotationally observed in astronomical environments than the other anion isomer unless physical or chemical conditions dictate a difference in the products. In such a case, SNO^- would be a marker for such conditions and would help to classify the astronomical regions in which it is found.

C. Vibrational frequencies

The CcCR harmonic vibrational frequencies for both SNO^- and OSN^- are in line with those determined from work by Trabelsi and co-workers,[3] indicating that the subsequent anharmonic frequencies should be well-behaved. The cubic and quadratic force constants for both anions are of a similar magnitude as those from the corresponding neutral radicals where the resulting VPT2-determined vibrational frequencies in the radical correlate quite well to experimental, condensed-phase values.[2] As a result, the anharmonic frequencies reported herein for SNO^- and OSN^- give no indication of being any less trustworthy than their corresponding radicals, and may even be more so since the anions are closed-shell species. The vibrational data produced in this study serve to further enhance the analysis of these simple anions.

The ω_1 N–O stretch of SNO^- is the brightest mode at 531 km/mol, as it was for SNO radical, as well, but the intensity of the ω_3 N–S stretch is significantly brighter for SNO^- (257 km/mol), where it was an order of magnitude dimmer in the radical. This trend also continues for OSN^- where the ω_1 "antisymmetric" stretch is 351 km/mol and the ω_3 "symmetric" stretch is 216 km/mol. The mode descriptions are discussed in more detail below. The ω_3 mode is brighter than the 31 km/mol ω_2 bend which was not the case in the corresponding OSN radical.

The SNO^- anharmonic fundamentals given in Table IV are understandably lower than the radical, again, from the behavior of the force constants compared between the radical and negatively charged species. There also are no large anharmonicities in any of these fundamentals as is most evident for the meager 5.4 cm^{-1} decrease in the zero-point frequency shift from harmonics (1304.3 cm^{-1}) to anharmonics (1298.6 cm^{-1}). Even though the overtones and combination bands are known to vary from experiment to a greater extent than the fundamentals,[72] the small anharmonicities present in the fundamentals should ensure that these frequencies are strong representations of physical reality. Inclusion of the isotopologues expectedly decreases each of the fundamental modes, especially for ^{15}N on the central atom reducing the stretches from 1336.1 cm^{-1} and 733 cm^{-1} to 1313.5 cm^{-1} and 714.2 cm^{-1}. Terminal isotopic substitution largely only affects the modes where these atoms are specifically included. As a result, the vibrational data for SNO^- are performing in a similar fashion as that known to provide good correlation to experiment. Such is expected for this anion, as well.

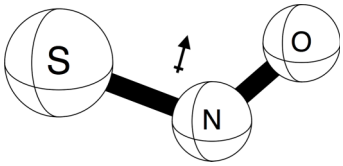

FIG. 1. The SNO^- CcCR equilibrium geometry and dipole moment vector.

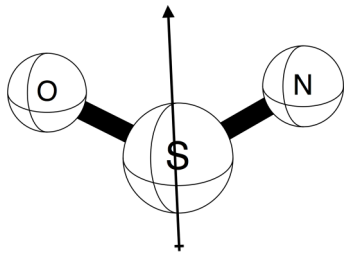

FIG. 2. The OSN^- CcCR equilibrium geometry and dipole moment vector.

The same conclusions about the expectations for the vibrational data of OSN^- given in Table V also hold true. The zero-point energy drops from 1401.5 cm^{-1} for the harmonic approximation to 1395.6 cm^{-1} for the quartic anharmonic, a decrease of only 5.9 cm^{-1}. This is roughly 100 cm^{-1} above the zero-point vibrational energy for SNO^-. The increase is largely attributable to the shift in vibrational behavior for the stretches caused by the similarity of the terminal atoms in OSN^-. As with the neutral radical,[2] the closeness of the nitrogen and oxygen masses creates "symmetric-" and "antisymmetric-"like vibrational behavior. The decrease of the ν_1 frequency with respect to SNO^- to 1280.2 cm^{-1} and the increase of the ν_3 frequency to 999.4 cm^{-1} giving a difference of 280.8 cm^{-1} are clear indicators that these motions are more concerted than in other systems such as SNO^-. As a consequence, the stretching behavior is akin to the stretching frequencies of isoelectronic, neutral SO_2 where the difference in stretching frequencies is in the 210 cm^{-1} range.[73] The overtones and combination bands are well-behaved, as are the frequencies of the isotopologues, again, supporting the precision and subsequent expected accuracy of these motions for OSN^-.

IV. CONCLUSIONS

The SNO^- and OSN^- anion isomers are shown here to be stable, well-behaved charged species performing in line with very recent work.[3] The geometry of SNO^- and its subsequent spectroscopic and vibrational properties differs notably from the neutral radical largely resulting from weaker bond strengths and a smaller bond angle. OSN^- does not change drastically for inclusion of the extra electron in the anion due to the centrality of the larger sulfur atom. Both molecules have bright stretching modes, but OSN^- will be more rotationally bright than SNO^- from the computed dipole moments and the lower relative energy. The eBEs computed are lower than those determined from recent computations, but they are qualitatively consistent. SNO^- and OSN^- cannot form from dipole-bound processes due to the small dipole moments in the neutral radicals but could still be present in atmospheric and astronomical environments since they are such stable, small species likely created from various other means and reactions. The spectroscopic data provided here all assist in observations of these systems whether in the laboratory or in space.

ACKNOWLEDGMENTS

R.C.F. acknowledges Georgia Southern University for providing start-up funds for this work. The authors also acknowledge Professor T. Daniel Crawford of Virginia Tech for the use of computer hardware.

[1]O. Yazidi, A. B. Houria, J. S. Francisco, and M. Hochlaf, J. Chem. Phys. **138**, 104318 (2013).
[2]R. C. Fortenberry and J. S. Francisco, J. Chem. Phys. **143**, 084308 (2015).
[3]T. Trabelsi, O. Yazidi, J. S. Francisco, R. Linguerri, and M. Hochlaf, J. Chem. Phys. **143**, 164301 (2015).
[4]V. A. Krasnopolsky, Icarus **191**, 25 (2007).
[5]V. A. Krasnopolsky, Icarus **218**, 230 (2012).
[6]P. O. Tchir and R. D. Spratley, Can. J. Chem. **53**, 2318 (1975).
[7]P. O. Tchir and R. D. Spratley, Can. J. Chem. **53**, 2331 (1975).
[8]M. Hawkins and A. J. Downs, J. Phys. Chem. **88**, 3042 (1984).
[9]L. Andrews, P. Hassanzadeh, G. D. Brabson, A. Citra, and M. Neurock, J. Phys. Chem. **100**, 8273 (1996).
[10]M. Bahou and Y. P. Lee, J. Chem. Phys. **115**, 10694 (2001).
[11]A. Gourmi, D. D. Shao, and P. Marshall, J. Chem. Phys. **121**, 9999 (2004).
[12]M. Méndez, J. S. Francisco, and D. A. Dixon, Chem. Eur. J. **20**, 10231 (2014).
[13]M. C. McCarthy, C. A. Gottlieb, H. Gupta, and P. Thaddeus, Astrophys. J. **652**, L141 (2006).
[14]J. Cernicharo, M. Guèlin, M. Agùndez, K. Kawaguchi, M. McCarthy, and P. Thaddeus, Astron. Astrophys. **467**, L37 (2007).
[15]S. Brünken, H. Gupta, C. A. Gottlieb, M. C. McCarthy, and P. Thaddeus, Astrophys. J. **664**, L43 (2007).
[16]A. J. Remijan, J. M. Hollis, F. J. Lovas, M. A. Cordiner, T. J. Millar, A. J. Markwick-Kemper, and P. R. Jewell, Astrophys. J. **664**, L47 (2007).
[17]P. Thaddeus, C. A. Gottlieb, H. Gupta, S. Brünken, M. C. McCarthy, M. Agùndez, M. Guèlin, and J. Cernicharo, Astrophys. J. **677**, 1132 (2008).
[18]M. Agúndez, J. Cernicharo, M. Guélin, M. Gerin, M. C. McCarthy, and P. Thaddeus, Astron. Astrophys. **478**, L19 (2008).
[19]J. Cernicharo, M. Guèlin, M. Agundez, M. C. McCarthy, and P. Thaddeus, Astrophys. J. **688**, L83 (2008).
[20]M. Agùndez, J. Cernicharo, M. Guèlin, C. Kahane, E. Roueff, J. Klos, F. J. Aoiz, F. Lique, N. Marcelino, J. R. Goicoechea, M. Gonzàlez Garcia, C. A. Gottlieb, M. C. McCarthy, and P. Thaddeus, Astron. Astrophys. **517**, L2 (2010).
[21]M. A. Cordiner, S. B. Charnley, J. V. Buckle, C. Walsh, and T. J. Millar, Astrophys. J. Lett. **730**, L18 (2011).
[22]M. A. Cordiner, J. V. Buckle, E. S. Wirström, A. O. H. Olofsson, and S. B. Charnley, Astrophys. J. **770**, 48 (2013).
[23]F. Carelli, F. A. Gianturco, R. Wester, and M. Satta, J. Chem. Phys. **141**, 054302 (2014).
[24]R. C. Fortenberry, J. Phys. Chem. A **119**, 9941 (2015).
[25]M. L. Theis, A. Candian, A. G. G. M. Tielens, T. J. Lee, and R. C. Fortenberry, Phys. Chem. Chem. Phys. **17**, 14761 (2015).
[26]C. Meredith, R. D. Davy, G. E. Quelch, and H. F. Schaefer III, J. Chem. Phys. **94**, 1317 (1990).
[27]W. Kutzelnigg, Angew. Chem., Int. Ed. Engl. **23**, 272 (1984).
[28]M. Driess and H. Grützmacher, Angew. Chem., Int. Ed. Engl. **35**, 828 (1996).
[29]D. E. Woon and T. H. Dunning, Comput. Theor. Chem. **963**, 7 (2011).
[30]R. C. Fortenberry, X. Huang, A. Yachmenev, W. Thiel, and T. J. Lee, Chem. Phys. Lett. **574**, 1 (2013).
[31]X. Huang and T. J. Lee, J. Chem. Phys. **129**, 044312 (2008).
[32]X. Huang and T. J. Lee, J. Chem. Phys. **131**, 104301 (2009).
[33]X. Huang, P. R. Taylor, and T. J. Lee, J. Phys. Chem. A **115**, 5005 (2011).
[34]R. C. Fortenberry, X. Huang, J. S. Francisco, T. D. Crawford, and T. J. Lee, J. Chem. Phys. **135**, 134301 (2011).
[35]R. C. Fortenberry, X. Huang, J. S. Francisco, T. D. Crawford, and T. J. Lee, J. Chem. Phys. **136**, 234309 (2012).
[36]R. C. Fortenberry, X. Huang, J. S. Francisco, T. D. Crawford, and T. J. Lee, J. Phys. Chem. A. **116**, 9582 (2012).
[37]X. Huang, R. C. Fortenberry, and T. J. Lee, J. Chem. Phys. **139**, 084313 (2013).
[38]D. Zhao, K. D. Doney, and H. Linnartz, Astrophys. J. Lett. **791**, L28 (2014).
[39]R. C. Fortenberry, X. Huang, T. D. Crawford, and T. J. Lee, J. Phys. Chem. A **118**, 7034 (2014).
[40]R. C. Fortenberry, X. Huang, J. S. Francisco, T. D. Crawford, and T. J. Lee, J. Chem. Phys. **135**, 214303 (2011).
[41]R. C. Fortenberry, X. Huang, T. D. Crawford, and T. J. Lee, Astrophys. J. **772**, 39 (2013).
[42]R. C. Fortenberry, T. D. Crawford, and T. J. Lee, Astrophys. J. **762**, 121 (2013).
[43]R. C. Fortenberry, X. Huang, T. D. Crawford, and T. J. Lee, Astrophys. J. **796**, 139 (2014).
[44]R. C. Fortenberry and T. J. Lee, Mol. Phys. **113**, 2012 (2015).
[45]W. J. Morgan and R. C. Fortenberry, J. Phys. Chem. A **119**, 7013 (2015).
[46]R. C. Fortenberry and J. A. Lukemire, Mon. Not. R. Astron. Soc. **453**, 2824 (2015).
[47]R. C. Fortenberry and R. Thackston, Int. J. Quantum Chem. **115**, 1650 (2015).
[48]P. Botschwina and R. Oswald, J. Chem. Phys. **129**, 044305 (2008).
[49]K. D. Jordan and F. Wang, Annu. Rev. Phys. Chem. **54**, 367 (2003).
[50]J. Simons, Annu. Rev. Phys. Chem. **62**, 107 (2011).
[51]A. C. Scheiner, G. E. Scuseria, J. E. Rice, T. J. Lee, and H. F. Schaefer III, J. Chem. Phys. **87**, 5361 (1987).
[52]K. Raghavachari, G. W. Trucks, J. A. Pople, and M. Head-Gordon, Chem. Phys. Lett. **157**, 479 (1989).

[53]T. H. Dunning, J. Chem. Phys. **90**, 1007 (1989).
[54]R. A. Kendall, T. H. Dunning, and R. J. Harrison, J. Chem. Phys. **96**, 6796 (1992).
[55]J. M. L. Martin and P. R. Taylor, Chem. Phys. Lett. **225**, 473 (1994).
[56]R. C. Fortenberry, X. Huang, T. D. Crawford, and T. J. Lee, J. Phys. Chem. A **117**, 9324 (2013).
[57]R. C. Fortenberry, T. D. Crawford, and T. J. Lee, J. Phys. Chem. A **117**, 11339 (2013).
[58]W. J. Morgan and R. C. Fortenberry, Spectrochim. Acta, Part A **135**, 965 (2015).
[59]H.-J. Werner, P. J. Knowles, F. R. Manby, M. Schütz, P. Celani, G. Knizia, T. Korona, R. Lindh, A. Mitrushenkov, G. Rauhut, T. B. Adler, R. D. Amos, A. Bernhardsson, A. Berning, D. L. Cooper, M. J. O. Deegan, A. J. Dobbyn, F. Eckert, E. Goll, C. Hampel, A. Hesselmann, G. Hetzer, T. Hrenar, G. Jansen, C. Köppl, Y. Liu, A. W. Lloyd, R. A. Mata, A. J. May, S. J. McNicholas, W. Meyer, M. E. Mura, A. Nicklass, P. Palmieri, K. Pflüger, R. Pitzer, M. Reiher, T. Shiozaki, H. Stoll, A. J. Stone, R. Tarroni, T. Thorsteinsson, M. Wang, and A. Wolf, MOLPRO, version 2010.1, a package of *ab initio* programs, 2010, see http://www.molpro.net.
[60]C. Møller and M. S. Plesset, Phys. Rev. **46**, 618 (1934).
[61]W. J. Hehre, R. Ditchfeld, and J. A. Pople, J. Chem. Phys. **56**, 2257 (1972).
[62]M. J. Frisch, G. W. Trucks, H. B. Schlegel, G. E. Scuseria, M. A. Robb, J. R. Cheeseman, G. Scalmani, V. Barone, B. Mennucci, G. A. Petersson, H. Nakatsuji, M. Caricato, X. Li, H. P. Hratchian, A. F. Izmaylov, J. Bloino, G. Zheng, J. L. Sonnenberg, M. Hada, M. Ehara, K. Toyota, R. Fukuda, J. Hasegawa, M. Ishida, T. Nakajima, Y. Honda, O. Kitao, H. Nakai, T. Vreven, J. A. Montgomery, Jr., J. E. Peralta, F. Ogliaro, M. Bearpark, J. J. Heyd, E. Brothers, K. N. Kudin, V. N. Staroverov, R. Kobayashi, J. Normand, K. Raghavachari, A. Rendell, J. C. Burant, S. S. Iyengar, J. Tomasi, M. Cossi, N. Rega, J. M. Millam, M. Klene, J. E. Knox, J. B. Cross, V. Bakken, C. Adamo, J. Jaramillo, R. Gomperts, R. E. Stratmann, O. Yazyev, A. J. Austin, R. Cammi, C. Pomelli, J. W. Ochterski, R. L. Martin, K. Morokuma, V. G. Zakrzewski, G. A. Voth, P. Salvador, J. J. Dannenberg, S. Dapprich, A. D. Daniels, O. Farkas, J. B. Foresman, J. V. Ortiz, J. Cioslowski, and D. J. Fox, GAUSSIAN 09 Revision D.01, Gaussian, Inc., Wallingford, CT, 2009.
[63]J. M. L. Martin and T. J. Lee, Chem. Phys. Lett. **258**, 136 (1996).
[64]M. Douglas and N. Kroll, Ann. Phys. **82**, 89 (1974).
[65]W. D. Allen *et al.*, *INTDER* 2005 is a general program written by W. D. Allen *et al.* which performs vibrational analysis and higher-order non-linear transformations, 2005.
[66]D. Papousek and M. R. Aliev, *Molecular Vibration-Rotation Spectra* (Elsevier, Amsterdam, 1982).
[67]I. M. Mills, in *Molecular Spectroscopy - Modern Research*, edited by K. N. Rao and C. W. Mathews (Academic Press, New York, 1972), pp. 115–140.
[68]J. K. G. Watson, in *Vibrational Spectra and Structure*, edited by J. R. During (Elsevier, Amsterdam, 1977), pp. 1–89.
[69]J. F. Gaw, A. Willets, W. H. Green, and N. C. Handy, in *Advances in Molecular Vibrations and Collision Dynamics*, edited by J. M. Bowman and M. A. Ratner (JAI Press, Inc., Greenwich, CT, 1991), pp. 170–185.
[70]R. C. Fortenberry and T. D. Crawford, J. Chem. Phys. **134**, 154304 (2011).
[71]J. Simons, J. Phys. Chem. A **112**, 6401 (2008).
[72]X. Huang, R. C. Fortenberry, Y. Wang, J. S. Francisco, T. D. Crawford, J. M. Bowman, and T. J. Lee, J. Phys. Chem. A **117**, 6932 (2013).
[73]R. C. Fortenberry, X. Huang, D. W. Schwenke, and T. J. Lee, Spectrochim. Acta, Part A **119**, 76 (2014).